Automotive Gas Turbine Regulation

R. Whalley and M. Ebrahimi

***Abstract*—A multivariable model of an automotive gas turbine, obtained from the linearized system equations is investigated. To facilitate vehicle speed changes, whilst protecting the system against thermal damage, control of the power turbine inlet gas temperature and gas generator speed is proposed by feedback regulation. Fuel flow and the power turbine nozzle area variations are the selected, manipulatable inputs. Owing to the limited control energy available for regulation purposes a multivariable, optimum, minimum control effort strategy is employed in the inner loop controller design study. Simulated, open and closed loop system responses are presented for purposes of comparison. Significant improvements in the transient response interaction reaction times and low steady state output interaction achieved using passive compensation and output feedback alone. Simplification of the closed loop configuration is proposed in the final implementation without performance penalties.**

***Index Terms*—Automotive, control, gas-turbine, optimum.**

NOMENCLATURE

$\mathbf{A}(\mathrm{s})$	Numerator of $\mathbf{G}(\mathrm{s})$ matrix.
$\mathrm{a_{ij}}(\mathrm{s})$	Element of $\mathbf{A}(\mathrm{s})$ function.
$\mathrm{a_{ij}}, \mathrm{b_{ij}}, \ldots \gamma_{\mathrm{ij}}$	Coefficients of $\mathrm{a_{ij}}(\mathrm{s})$ scalar.
$\mathrm{b}(\mathrm{s})$	Polynomial function.
b_0	Leading coefficient of $\mathrm{b}(\mathrm{s})$ scalar.
$\mathrm{d}(\mathrm{s})$	Denominator of $\mathbf{G}(\mathrm{s})$ function.
$\mathrm{f}(\mathrm{s})$	Transformed fuel flow signal scalar.
$f_1(\mathrm{s}), f_1(\mathrm{s}),$	Outer loop filters function.
$\bar{\mathbf{G}}(\mathrm{s})$	Transfer function array matrix.
$\mathbf{G}(\mathrm{s})$	Transfer function array for analysis matrix.
$\mathbf{G}_{\mathrm{P}}(\mathrm{s})$	Uncompensated system model matrix.
$\mathrm{g_{ij}}(\mathrm{s})$	Elements of $\mathbf{G}(\mathrm{s}), 1 \leq \mathrm{i}, \mathrm{j} \leq \mathrm{m}$ function.
$\mathrm{h_j}(\mathrm{s})$	Transformed feedback path compensator $1 \leq \mathrm{j} \leq 2$ function.
$\mathbf{I}$	Identity matrix matrix.
$\mathbf{J}$	Performance index functional.
$\mathrm{k_j}(\mathrm{s})$	Transformed forward path compensator $1 \leq \mathrm{j} \leq \mathrm{m}$function.
$\mathrm{k}_1, \mathrm{k}_2, \ldots, \mathrm{k_m}$	Gains of $\mathrm{k_j}(\mathrm{s}), 1 \leq \mathrm{i}, \mathrm{j} \leq \mathrm{m}$ scalar.
$\mathrm{h}_1, \mathrm{h}_2, \ldots, \mathrm{h_m}$	Gains of $\mathrm{h_j}(\mathrm{s}), 1 \leq \mathrm{i}, \mathrm{j} \leq \mathrm{m}$ scalar.
$\mathbf{L}(\mathrm{s})$	Left row factors matrix.
m	Number of inputs and outputs scalar.
$\mathrm{n}(\mathrm{s})$	transformed nozzle actuator signal scalar.
$\mathrm{n}, \mathrm{n}_1, \mathrm{n}_2, \ldots, \mathrm{n_{m-1}}$	Gain ratios scalar.
$\mathbf{P}(\mathrm{s})$	Pre-compensator matrix
$\mathbf{Q}$	Coefficient array matrix.
$\mathrm{r}(\mathrm{s})$	Transformed reference input function.
$\mathbf{R}(\mathrm{s})$	Right column factors matrix.
$\mathrm{R}_1, \mathrm{R}_2$	Reference input gains scalar.
$\mathrm{T}(\mathrm{s})$	Transformed gas temperature signal scalar.
$\omega(\mathrm{s})$	Transformed gas turbine speed signal scalar.
$\mathbf{u}(\mathrm{s})$	Transformed input vector.
$\mathbf{y}(\mathrm{s})$	Transformed output vector.
H_∞	Hardy space space.
$\Gamma(\mathrm{s})$	Finite time delays matrix.
κ	Degree of $\mathrm{d}(\mathrm{s})$ scalar.
τ	Gas turbine time constant scalar.
$\delta(\mathrm{s})$	Disturbances vector.

Manuscript received March 26, 2002; revised December 17, 2002. Manuscript received in final form May 27, 2003. Recommended by Associate Editor A. Ray.

The authors are with the School of Engineering, Design and Technology, University of Bradford, West Yorkshire BD7 1DP, U.K. (e-mail: m.ebrahimi@bradford.ac.uk).

Digital Object Identifier 10.1109/TCST.2004.824336

I. INTRODUCTION

TRIALS on automotive gas turbines have been conducted for over two decades in order to develop this system and demonstrate effectiveness. In particular, the possibility of providing an alternative to diesel engine propulsion for "large" road vehicles has been a much stated aim [1], enabling higher vehicle power-weight-ratios, improved reliability and lower maintenance costs to be attained.

In this respect gas turbine propulsion must eclipse the efficiency and cost effectiveness commanded by internal combustion engines. Moreover, the driving controls must be analogous to those for existing prime movers wherein increases and reductions in power are achieved via increases or reductions in the angle of an accelerator pedal.

Although the part-load efficiency of gas turbine plant is "poor" the advantages of this prime mover in terms of its power to weight ratio and compactness are impressive. Additionally, the low cost of these units, once they are provided by volume manufacturing, their reliability and vibration free performance are all attractive features.

To improve fuel efficiency, at less than full load, automotive gas turbines have variable geometry, power turbine nozzles. This enables the gas temperature, at the inlet to the power turbine, to be maintained at "high levels" increasing efficiency and reducing fuel consumption thereby.

Automotive gas turbine power plant have therefore manipulatable inputs, which comprise the power turbine nozzle area and the fuel flow rate to the combustion chambers. The outputs, which are to be regulated, are the gas temperature at the nozzle exit, since the power output from the system is proportional to its cube, and gas generator speed, as discussed in [2].

A typical automotive gas turbine arrangement is shown in Fig. 1. Essentially, air entering the system is compressed, passed

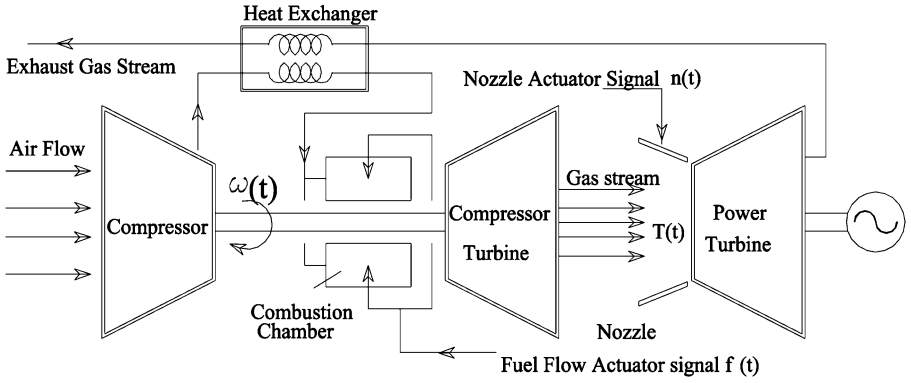

Fig. 1. Arrangement of automotive gas turbine.

through a heat exchanger, enabling a further increase in temperature from the exhaust gas stream to be obtained, before entering the combustion chambers. Fuel is continuously injected into these chambers and the resulting hot gas is expanded, first through the compressor turbine and then through the power turbine via a variable orifice nozzle.

In this application the output variables to be regulated are the gas generator speed and the temperature of the gas stream entering the power turbine, which dictates the vehicle speed. Moreover, the gas stream temperature excursions have to be confined in order to prevent creep and blade damage.

In order to effect regulation the fuel flow to the combustion chamber may be varied and this will alter both the gas stream temperature and the gas generator turbine and compressor speed. Similarly the gas stream nozzle area may be altered. This also changes the gas temperature and the power output rendering the system model highly interactive. Further details of compact general purpose gas turbines are given in [3].

The linearized model of the system forms a two input—two output, multivariable system. To design a minimum control effort, multivariable controller for this process the theoretical details given in Section II must be followed. Importantly, this controller also exploits the naturally occurring high gain channels of the system model ensuring that low feedback gains and economical implementation are achieved thereby.

II. Closed-Loop Analysis

Automotive gas turbine models may be represented by an input-output relationship. Herein, the general transformed, precompensated system models employed are assumed to be linear, finite dimensional, and time invariant realizations, in the Laplace variable s, denoted by $\mathbf{G}(\mathrm{s})$ where

$$\mathbf{G}(\mathrm{s}) = \mathbf{G}_{\mathrm{p}}(\mathrm{s})\mathbf{P}(\mathrm{s})\Gamma(\mathrm{s}).$$

Models with m inputs and m outputs, admit a rational, factorization

$$\mathbf{G}(\mathrm{s}) = \mathbf{L}(\mathrm{s})\frac{\mathbf{A}(\mathrm{s})}{\mathrm{d}(\mathrm{s})}\mathbf{R}(\mathrm{s})\Gamma(\mathrm{s}) \tag{1}$$

where

$$\mathbf{L}(\mathrm{s}), \mathbf{A}(\mathrm{s}), \mathbf{R}(\mathrm{s}), \Gamma(\mathrm{s}) \quad \text{and} \quad \mathrm{d}(\mathrm{s}) \in H_\infty$$

and:

$$\mathbf{L}(\mathrm{s})\frac{\mathbf{A}(\mathrm{s})}{\mathrm{d}(\mathrm{s})}\mathbf{R}(\mathrm{s}) = \mathbf{G}_{\mathrm{p}}(\mathrm{s})\mathbf{P}(\mathrm{s})$$

In (1), $\mathbf{L}(\mathrm{s})$ contains the left (row) factors, $\mathbf{R}(\mathrm{s})$ contains the right (column) factors and $\Gamma(\mathrm{s})$ contains the transformed, actuator finite time delays of $\mathbf{G}(\mathrm{s})$ such that the $\mathrm{m} \times \mathrm{m}$ matrices comprising 1 are

$$\mathbf{L}(\mathrm{s}) = \mathrm{Diag}(\lambda_{\mathrm{j}}(\mathrm{s})/\mathrm{p}_{\mathrm{j}}(\mathrm{s})), \quad \mathbf{R}(\mathrm{s}) = \mathrm{Diag}(\rho_{\mathrm{j}}(\mathrm{s})/\mathrm{q}_{\mathrm{j}}(\mathrm{s}))$$
$$\Gamma(\mathrm{s}) = \mathrm{Diag}(\mathrm{e}^{-\mathrm{sT_j}}) \quad 1 \le \mathrm{j} \le \mathrm{m}$$

and $\mathbf{A}(\mathrm{s})$ is a matrix of rational function, such that $\det \mathbf{A}(\mathrm{s}) \neq 0$, with elements

$$\mathrm{a_{ij}}(\mathrm{s}) = \mathrm{a_{ij}}\mathrm{s}^{\mathrm{m}-1} + \mathrm{b_{ij}}\mathrm{s}^{\mathrm{m}-2} + \cdots \gamma_{\mathrm{ij}}, \quad 1 \le \mathrm{i}, \mathrm{j} \le \mathrm{m}. \tag{2}$$

The transformed input–output disturbance relationship is therefore

$$\mathbf{y}(\mathrm{s}) = \mathbf{G}(\mathrm{s})\mathbf{u}(\mathrm{s}) + \delta(\mathrm{s}). \tag{3}$$

If the inner loop control law is

$$\mathbf{u}(\mathrm{s}) = \mathbf{k}(\mathrm{s})(\mathrm{r}(\mathrm{s}) - \mathbf{h}(\mathrm{s})\mathbf{y}(\mathrm{s})) \tag{4}$$

then combining (3) and (4) yields

$$\mathbf{y}(\mathrm{s}) = (\mathbf{I} + \mathbf{G}(\mathrm{s})\mathbf{k}(\mathrm{s})\mathbf{h}(\mathrm{s}))^{-1}(\mathbf{G}(\mathrm{s})\mathbf{k}(\mathrm{s})\mathrm{r}(\mathrm{s}) + \delta(\mathrm{s})). \tag{5}$$

The finite time delays in $\Gamma(\mathrm{s})$ may be ordered with: $\mathrm{T_i} \ge \mathrm{T_j}, 1 \le \mathrm{j} \le \mathrm{m}\, \mathrm{i} \neq \mathrm{j}$, so that the forward path gain vector can be arranged as

$$\mathbf{k}(\mathrm{s}) = \Big[\mathrm{k}_1(\mathrm{s})\mathrm{e}^{-\mathrm{s}(\mathrm{T_i}-\mathrm{T}_1)}, \mathrm{k}_2(\mathrm{s})\mathrm{e}^{-\mathrm{s}(\mathrm{T_i}-\mathrm{T}_2)} \cdots \mathrm{k_i}(\mathrm{s})\mathrm{e}^{-\mathrm{sT_i}} \cdots \mathrm{k_m}(\mathrm{s})\mathrm{e}^{-\mathrm{s}(\mathrm{T_i}-\mathrm{T_m})}\Big]^{\mathrm{T}} \tag{6}$$

and since

$$\mathbf{h}(\mathrm{s}) = (\mathrm{h}_1(\mathrm{s}), \mathrm{h}_2(\mathrm{s}) \cdots \mathrm{h_m}(\mathrm{s})) \tag{7}$$

then if

$$\mathrm{k_j}(\mathrm{s}) = \mathrm{k_j}\phi_{\mathrm{j}}(\mathrm{s}) \quad \text{and} \quad \mathrm{h_j}(\mathrm{s}) = \mathrm{h_j}\chi_{\mathrm{j}}(\mathrm{s}) \quad 1 \le \mathrm{j} \le \mathrm{m}$$

where $\phi_j(s)$ and $\chi_j(s)$ are proper or strictly proper, stable, realizable, minimum phase, rational functions then they may be selected such that (5) becomes

$$\mathbf{y}(s) = \left(\mathbf{I} + \frac{e^{-sT_i} n(s)\mathbf{A}(s)\mathbf{kh}}{d(s)}\right)^{-1} \times \left(\frac{n(s)\mathbf{A}(s)\mathbf{k}e^{-sT_i} r(s)}{d(s)} + \boldsymbol{\delta}(s)\right) \quad (8)$$

where in (8)

$$\mathbf{k} = (k_1, k_2 \ldots k_m)^T \quad (9)$$

$$\mathbf{h} = (h_1, h_2 \ldots h_m) \quad (10)$$

$$d(s) = s^\kappa + a_1 s^{\kappa-1} + \cdots a_0$$

and

$$\deg\left(n(s)a_{i,j}(s)\right) < \kappa. \quad 1 \le i, j \le m.$$

The determinant required in (8), as shown in [4] is

$$\det\left[\mathbf{I} + e^{-sT_i} n(s)\frac{\mathbf{A}(s)}{d(s)}\mathbf{kh}\right] = 1 + e^{-sT_i} n(s)\mathbf{h}\frac{\mathbf{A}(s)}{d(s)}\mathbf{k} \quad (11)$$

The inner product in (11) may be expressed as

$$\mathbf{hA}(s)\mathbf{k} = [1, s, \ldots s^{m-1}] \times \begin{bmatrix} \gamma_{11} & \gamma_{12} & \cdots & \gamma_{mm} \\ \vdots & \vdots & & \vdots \\ b_{11} & b_{12} & \cdots & b_{mm} \\ a_{11} & a_{12} & \cdots & a_{mm} \end{bmatrix} \begin{bmatrix} k_1 h_1 \\ k_2 h_1 \\ \vdots \\ k_m h_m \end{bmatrix}. \quad (12)$$

If in (12) the gain ratios are

$$k_2 = n_1 k_1, \quad k_3 = n_2 k_1, \ldots k_m = n_{m-1} k_m \quad (13)$$

and:

$$\mathbf{hA}(s)\mathbf{k} = \mathbf{b}(s) \quad (14)$$

then (14) implies that

$$k_1[\mathbf{Q}]\mathbf{h} = (b_m, b_{m-1}, \ldots, b_0)^T \quad (15)$$

where in (15)

$$\mathbf{Q} = \begin{bmatrix} q_{1,1} & q_{1,2} & \cdots & q_{1,m} \\ \vdots & \vdots & \cdots & \vdots \\ q_{m-1,1} & q_{m-1,2} & \cdots & q_{m-1,m} \\ q_{m,1} & q_{m,2} & \cdots & q_{m,m} \end{bmatrix}$$

$$q_{1,1} = \gamma_{11} + \gamma_{12} n_1 + \cdots \gamma_{1m} n_{m-1}$$
$$q_{1,2} = \gamma_{21} + \gamma_{22} n_1 + \cdots \gamma_{2m} n_{m-1}$$
$$q_{m-1,1} = b_{11} + b_{12} n_1 + \cdots b_{1m} n_{m-1}$$
$$q_{m-1,2} = b_{21} + b_{22} n_1 + \cdots b_{2m} n_{m-1}$$
$$q_{m,1} = a_{11} + a_{12} n_1 + \cdots a_{1m} n_{m-1}$$
$$q_{m,2} = a_{21} + a_{22} n_1 + \cdots a_{2m} n_{m-1}$$
$$q_{1,m} = \gamma_{m1} + \gamma_{m2} n_1 + \cdots \gamma_{mm} n_{m-1}$$
$$q_{m-1,m} = b_{m1} + b_{m2} n_1 + \cdots a_{mm} n_{m-1}$$
$$q_{m,m} = a_{m1} + a_{m2} n_1 + \cdots a_{mm} n_{m-1}$$

and; $b_j, 0 \le j \le m$, are the coefficients of $b(s)$, given in (14). Providing $n_1, n_2 \cdots n_{m-1}$ can be selected in (15) so that the matrix is invertible then a unique solution for $(h_1, h_2, \ldots h_m)k_1$ exists.

III. Minimum Control Effort Analysis

Now that a route for analyzing closed loop systems, using the transfer function matrix and output measurements alone has been established, the possibility of optimizing this process can be considered. An indication that the freedom exists to do this arises from the arbitrary choice of n_1, n_2, etc. for the gain ratios.

Minimizing the control effort, to disturbance inputs, under closed loop conditions, with the restriction that the controller model generates a particular polynomial, would provide a useful result. This polynomial influences the migration pattern of the closed-loop poles so that control effort minimization to disturbances and the desired system response to input changes could be achieved simultaneously. The controller equation for a system having m inputs and m outputs is given by (3).

The control effort at time t, from (4), with $r(s) = 0$ is

$$\begin{aligned}&(|k_1 h_1| + |k_2 h_1| \cdots |k_m h_1|)|y_1(t)| \\ &\quad + (|k_1 h_2| + \cdots |k_m h_2|)|y_2(t)| \\ &\quad \cdots + (|k_1 h_m| + |k_2 h_m| + \cdots |k_m h_m|)|y_m(t)| \end{aligned} \quad (16)$$

then for arbitrary changes in the transformed output vector $\mathbf{y}(t)$, following arbitrary disturbance changes, minimizing:

$$J = \sum_{i=1}^{m} h_i^2 \sum_{j=1}^{m} k_j^2 \quad (17)$$

would minimize the control effort given by expression (16). If the relationships

$$k_2 = n_1 k_1, \quad k_3 = n_2 k_1, \ldots, k_m = n_{m-1} k_1$$

are adopted, then (17) can be written as

$$J = (k_1)^2 \left(1 + n_1^2 + n_2^2 \ldots n_{m-1}^2\right)\left(h_1^2 + h_2^2 \ldots h_m^2\right) \quad (18)$$

and $h_1^2 + h_2^2 \ldots h_m^2 = \langle h, h \rangle$. The closed-loop determinant is given by (11) with the inner product equated to $b(s)$, as in (14), then from (15)

$$\mathbf{h} = k_1^{-1}\mathbf{Q}^{-1}\mathbf{b}. \quad (19)$$

Upon substituting for $\mathbf{h}$ from (19), (18) becomes

$$J = \left(1 + n_1^2 + n_2^2 + \cdots n_{m-1}^2\right)\mathbf{b}^T(\mathbf{Q}^{-1})^T\mathbf{Q}^{-1}\mathbf{b}. \quad (20)$$

To find the concave minimum value for J, assuming, for example, that $m = 3$ gives

$$J = \left(1 + n_1^2 + n_2^2\right)\mathbf{b}^T\left(\mathbf{Q}^{-1}\right)^T\mathbf{Q}^{-1}\mathbf{b}$$

where J is minimized when

$$\frac{\partial J}{\partial n_1} = 0, \frac{\partial J}{\partial n_2} = 0 \quad \text{and} \quad \frac{\partial^2 J}{\partial n_1^2}\frac{\partial^2 J}{\partial n_2^2} - \left(\frac{\partial^2 J}{\partial n_1 \partial n_2}\right)^2 > 0$$

if $(\partial^2 J)/(\partial n_1^2) > 0$.

For $m > 3$ a numerical minimization routine would have to be employed to establish the values of $n_1, n_2 \ldots n_{m-1}$ which minimize J. There are many procedures available for this task

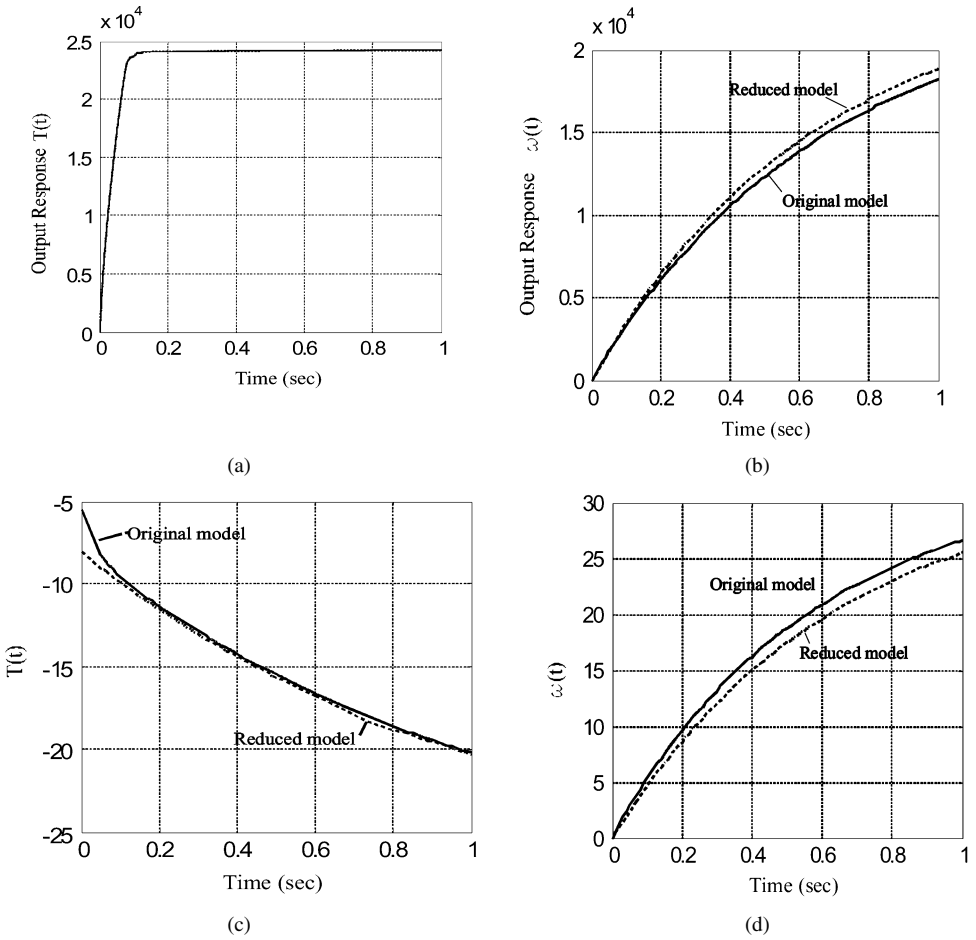

Fig. 2. (a) Temperature variation following a unit step change on the fuel flow. (b) Speed variation following a unit step change on the fuel flow. (c) Temperature variation following a unit step change on the nozzle area. (d) Speed variation following a unit step change on nozzle area.

as indicated by [5] with rapid convergence and high accuracy characteristics. This completes the analysis.

IV. Automotive Gas Turbine Model

Linearized, small signal models of automotive gas turbines, operating under specified load conditions, are presented in [1]–[3], [6]. The input vector for these transformed models is $\mathbf{u}(\mathrm{s})$ and the output vector is $\mathbf{y}(\mathrm{s})$ where

$$\mathbf{y}(\mathrm{s}) = \bar{\mathbf{G}}(\mathrm{s})\mathbf{u}(\mathrm{s}) \tag{21}$$

and in (21)

$$\mathbf{y}(\mathrm{s}) = [\mathrm{T}(\mathrm{s}), \omega(\mathrm{s})]^{\mathrm{T}}, \quad \mathrm{u}(\mathrm{s}) = [\mathrm{f}(\mathrm{s}), \mathrm{n}(\mathrm{s})]^{\mathrm{T}}$$

$$\bar{\mathbf{G}}(\mathrm{s}) = \begin{bmatrix} \mathrm{g}_1 & \mathrm{g}_{12} \\ \mathrm{g}_{21} & \mathrm{g}_{22} \end{bmatrix}$$

$$\mathrm{g}_{11} = \frac{1.3(\mathrm{s}+258.46)10^6}{(\mathrm{s}+39.4241)(\mathrm{s}+352.5758)}$$

$$\mathrm{g}_{12} = \frac{-5.6(\mathrm{s}+3.2674))(\mathrm{s}+40.6617)}{(\mathrm{s}+28.001)(\mathrm{s}+0.95)}$$

$$\mathrm{g}_{21} = \frac{9.04(\mathrm{s}+31.412)10^6}{(\mathrm{s}+187.3925)(\mathrm{s}+44.1697)(\mathrm{s}+44.1697)}$$

and

$$\mathrm{g}_{22} = \frac{83.4(\mathrm{s}+75.5395)}{(\mathrm{s}+113.2745)(\mathrm{s}+1.7214)}$$

Consequently, (21) relates the changes in the outputs of the transformed gas stream temperature $\mathrm{T}(\mathrm{s})$, as it enters the power turbine and the transformed gas generator speed $\omega(\mathrm{s})$ to the transformed fuel flow rate changes $\mathrm{f}(\mathrm{s})$ and the transformed nozzle area changes $\mathrm{n}(\mathrm{s})$. Disturbances owing to loading, environmental changes and internally generated shock and vibration also enter the system affecting both speed and the gas stream temperature variations. It is evident from (21) that the $\overline{\mathbf{G}}(\mathrm{s})$ matrix has many remote poles and zeros, which could be safely discounted without significantly affecting the design process. If these singularities are extracted, adjacent poles are combined and steady state conditions are maintained then the matrix model, for analysis purposes, becomes

$$\mathbf{G}(\mathrm{s}) = \begin{bmatrix} \frac{0.967.10^6}{\mathrm{s}+40.0} & \frac{-8.1248(\mathrm{s}+3.27)}{(\mathrm{s}+0.95)} \\ \frac{8.82\cdot10^6(\mathrm{s}+31.42)}{(\mathrm{s}+1.55)(\mathrm{s}+40)(\mathrm{s}+187.4)} & \frac{50.20}{(\mathrm{s}+1.55)} \end{bmatrix}. \tag{22}$$

Fig. 2(a)–(d) shows the transient responses for unit step input changes first on the fuel flow rate and then on the nozzle area. The full lines show the original model $\bar{\mathbf{G}}(\mathrm{s})$ transients while the dotted lines depict the reduced $\mathbf{G}(\mathrm{s})$ transients. As these responses indicate the differences in these characteristics are relatively small.

Consequently, the reduced model will be used in the controller design exercise. The procedure is sufficiently robust to allow this relaxation. Moreover, this will be demonstrated by

using the derived controller together with the original model in the final, digital simulation of the closed-loop system.

The objective of the regulation exercise is to improve the speed of response the system so that steady state conditions are achieved in less than 0.1 seconds. Commensurate with this aim the outputs should be substantially decoupled enabling the virtual adjustment of either output via independent, input reference, set point variations. These specification requirements should be attained whilst employing, inner-loop, minimum control effort in the suppression of arbitrary disturbances.

V. Determining the Closed-Loop Denominator

The transfer function matrix given by (22) can be arranged, following the extraction of row and column factors as

$$\mathbf{G}(\mathrm{s}) = \mathbf{L}(\mathrm{s})\mathbf{A}(\mathrm{s})\mathbf{R}(\mathrm{s}) \tag{23}$$

where in (23)

$$\mathbf{L}(\mathrm{s}) = \begin{bmatrix} \frac{1}{(\mathrm{s}+0.95)} & 0 \\ 0 & \frac{1}{(\mathrm{s}+1.55)(\mathrm{s}+187.4)} \end{bmatrix}$$

$$\mathbf{A}(\mathrm{s}) = \begin{bmatrix} 0.967(\mathrm{s}+0.95)10^6 & -8.1248(\mathrm{s}+3.27) \\ 8.82(\mathrm{s}+31.42)10^6 & 50.20(\mathrm{s}+187.4) \end{bmatrix}$$

and

$$\mathbf{R}(\mathrm{s}) = \begin{bmatrix} \frac{1}{(\mathrm{s}+40)} & 0 \\ 0 & 1 \end{bmatrix}$$

since in (5), with $\delta(\mathrm{s}) = 0$

$$\mathbf{y}(\mathrm{s}) = (\mathbf{I} + \mathbf{G}(\mathrm{s})\mathbf{k}(\mathrm{s})\mathbf{h}(\mathrm{s}))^{-1}\mathbf{G}\mathbf{k}(\mathrm{s})\mathrm{r}(\mathrm{s}) \tag{24}$$

and from (11) the determinant required in (24) is

$$\det(\mathbf{I} + \mathbf{G}(\mathrm{s})\mathbf{k}(\mathrm{s})\mathbf{h}(\mathrm{s})) = 1 + \mathbf{h}(\mathrm{s})\mathbf{G}(\mathrm{s})\mathbf{k}(\mathrm{s}) \tag{25}$$

where, in (25), if

$$\mathbf{h}(\mathrm{s}) = \left[\frac{(\mathrm{s}+0.95)\mathrm{h}_1}{(\mathrm{s}+1.55)(\mathrm{s}+187.4)}, \quad \mathrm{h}_2 \right] \tag{26}$$

and

$$\mathbf{k}(\mathrm{s}) = \begin{bmatrix} \left(\frac{\mathrm{s}+40}{\mathrm{s}+400}\right)\mathrm{k}_1 \\ \frac{\mathrm{k}_2}{\mathrm{s}+400} \end{bmatrix} \tag{27}$$

then the closed-loop characteristic equation from (25) becomes

$$0 = 1 + \frac{(\mathrm{h}_1, \mathrm{h}_2)\mathbf{A}(\mathrm{s})(\mathrm{k}_1, \mathrm{k}_2)^{\mathrm{T}}}{(\mathrm{s}+1.55)(\mathrm{s}+187.4)(\mathrm{s}+400)}. \tag{28}$$

If now the inner product of (28) in accordance with (14) is equated to a polynomial $\mathrm{b}(\mathrm{s})$ then

$$1 + \frac{\mathrm{b}(\mathrm{s})}{(\mathrm{s}+1.55)(\mathrm{s}+187.4)(\mathrm{s}+400)} = 0. \tag{29}$$

In (29) if $\mathrm{b}(\mathrm{s}) = \mathrm{sb}_0$, then with: $\mathrm{b}_0 = 2.6966.10^6$, the closed-loop poles are: $\mathrm{s} = -294 \pm 1638.8235\mathrm{i}, -0.0419$ and the dominant closed-loop pole is $\mathrm{s} = -0.0419$.

By selecting this pole configuration the dynamics of the two outputs become distinctly different enabling simple outer loop tuning, as shown later. Before this can be demonstrated the gains $\mathrm{k}_1, \mathrm{k}_2, \mathrm{h}_1$, and h_2 need to be determined from the optimization analysis in Section 6. This analysis enables these values to be calculated so that least control effort is required, for disturbance regulation purposes. Owing to the limited generator capacity, in automotive applications, where space and mass restrictions inhibit alternator size and hence the provision of strictly finite electrical energy supplies, this requirement becomes mandatory.

VI. Optimization

Equating the numerator of (28) to $\mathrm{b}(\mathrm{s})$ yields

$$[\mathrm{h}_1, \mathrm{h}_2]\mathbf{A}(\mathrm{s})[\mathrm{k}_1, \mathrm{k}_2]^{\mathrm{T}} = \mathrm{b}(\mathrm{s}). \tag{30}$$

Equation (30) can be expanded, as in (12) becoming

$$\begin{bmatrix} 0.918.10^6 & -26.5638 & 2772.2.10^5 & 9424.5 \\ 0.167.10^6 & -8.125 & 88.2.10^5 & 50.2 \end{bmatrix} \times \begin{bmatrix} \mathrm{k}_1\mathrm{h}_1 \\ \mathrm{k}_2\mathrm{h}_1 \\ \mathrm{k}_1\mathrm{h}_2 \\ \mathrm{k}_2\mathrm{h}_2 \end{bmatrix} = \begin{bmatrix} 0 \\ 1 \end{bmatrix} \mathrm{b}_0. \tag{31}$$

Putting $\mathrm{k}_2 = \mathrm{nk}_1$ in (31) gives, as in (15)

$$\mathrm{k}_1\mathbf{Q}\mathbf{h} = (0,1)^{\mathrm{T}} rmb_0 \tag{32}$$

where in (32), k_1 may be set to unity, so that

$$\mathbf{Q} = \begin{bmatrix} 0.918.10^6 - 26.5638\mathrm{n} & 2272.10^5 + 9424.5\mathrm{n} \\ 0.967.10^6 - 8.125\mathrm{n} & 88.2.10^5 + 50.2\mathrm{n} \end{bmatrix}$$

and since $\mathrm{b}_0 = 2.6966.10^6$, and if the performance index is defined as

$$\mathrm{J} = \sum_{\mathrm{i}=1}^{2} \mathrm{h}_{\mathrm{i}}^2 \sum_{\mathrm{j}=1}^{2} \mathrm{k}_{\mathrm{j}}^2$$

as in (17), then here

$$\mathrm{J} = (1+\mathrm{n}^2)\mathbf{b}^{\mathrm{T}}(\mathbf{Q}^{-1})^{\mathrm{T}}\mathbf{Q}^{-1}\mathbf{b} \tag{33}$$

where in (33), $\mathbf{b} = (0,1)^{\mathrm{T}} 2.6966.10^6$.

Expanding (33), following the substitution of $\mathbf{b}$ and $\mathbf{Q}$ yields (34) shown at the bottom of the page. Equation (34) is minimized when

$$\frac{\mathrm{dJ}}{\mathrm{dn}} = 0 \tag{35}$$

$$\mathrm{J} = \frac{4.5447.10^{11}(1+\mathrm{n}^2)(4.8805.10^{17}\mathrm{n}^2 + 2.8711.10^{22}\mathrm{n} + 4.2229.10^{26})}{(517.0\mathrm{n}^2 - 4.8445.10^7\mathrm{n} - 1.7865.10^{12})^2}. \tag{34}$$

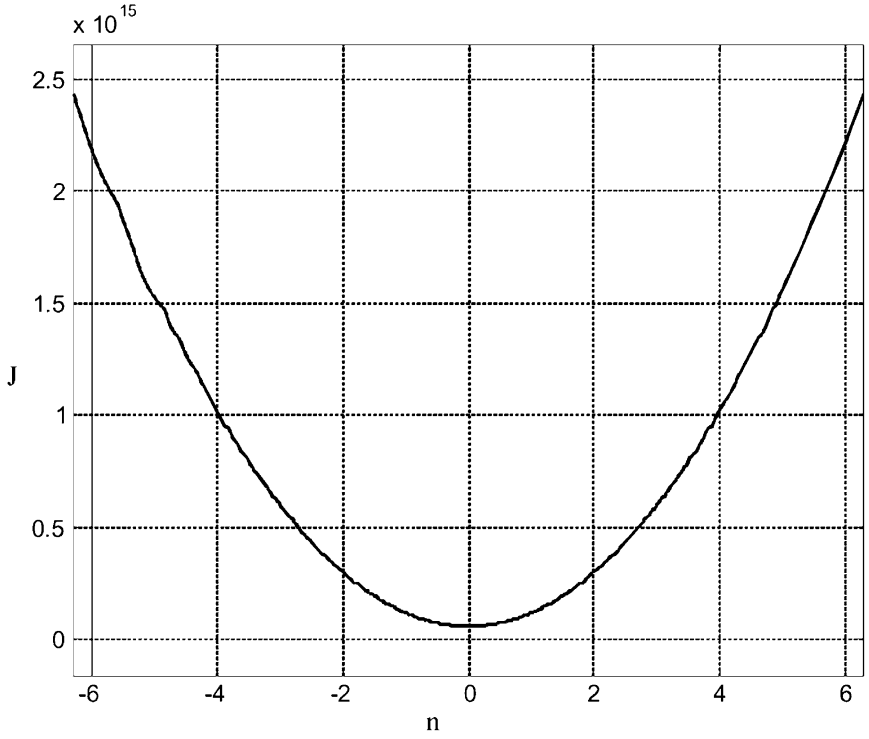

Fig. 3. Performance Index J against gain ratio n.

providing: $\mathrm{d}^2\mathrm{J}/\mathrm{dn}^2 > 0$. From (35) we show (36) the bottom of the page. From (36), the values of n which satisfy (35) are

$$\mathrm{n} = -29\,623.4, -27\,962.0 \pm 6142.0\mathrm{i} \quad \text{and} \quad -8.0.10^{-6}. \tag{37}$$

From the graph of J against n shown in Fig. 3 it is evident that the absolute minimum occurs when:

$$\mathrm{n} = -8.0.10^{-6}. \tag{38}$$

Upon substituting this value of n into (32) with $\mathrm{k}_1 = 1$ and $\mathrm{n} = -8.0.10^{-6}$

$$\mathrm{h} = \begin{bmatrix} 2.8757 \\ -0.0009 \end{bmatrix}. \tag{39}$$

Equations (26), (27), (38), and (39) fully define the feedback and forward path controller parameters completing thereby the inner loop closed-loop synthesis.

It is easy to show by calculating the inner, closed-loop transfer function of

$$\mathbf{y}(\mathrm{s}) = (\mathbf{I}_\mathrm{m} + \mathbf{G}(\mathrm{s})\mathbf{k}(\mathrm{s})\mathbf{h}(\mathrm{s}))^{-1}\mathbf{G}\mathbf{k}(\mathrm{s})\mathrm{r}(\mathrm{s})$$

that is shown in the equation at the bottom of the page.

For a unit step reference input changes on $\mathrm{r}(\mathrm{t})$, the system produces rapidly responding, increasing, oscillatory, temperature change transients and relatively slowly increasing, oscillatory, speed transients. The very large steady state excursions encountered, under open loop conditions, have also been contained now.

These responses are shown in Fig. 4 where the widely differing reaction times to quiescence are evident. Owing to these differences, simple outer loop controls can be employed to secure specified transient conditions with the steady-state output coupling being confined to less than 5.0%.

Simple passive filters may now be utilized to achieve the compensation required. This is discussed in Section VII.

VII. Tuning the Outer Loop

To obtain smooth, rapid, overdamped temperature changes a filter comprising two cascaded, simple delays of approximately 0.04 and 0.004 s were used together with a low, outer loop forward path gain of 0.04 giving $f_1(\mathrm{s}) = 0.04/(0.0002\mathrm{s}^2 + 0.05\mathrm{s} + 1)$. This calmed the rapid, oscillatory transient arising from the inner loop feedback whilst maintaining "low" output steady-state and transient coupling, as shown in Fig. 5(a). This was

$$\frac{\mathrm{dJ}}{\mathrm{dn}} = \frac{-0.9090.10^{12}(3.1070.10^{25}\mathrm{n}^4 + 2.6580.10^{30}\mathrm{n}^3 + 7.6940.10^{35}\mathrm{n}^2 + 7.544.10^{38}\mathrm{n} + 5.189.10^{33})}{(517.0\mathrm{n}^2 + 4.8445.10^{7}\mathrm{n} - 1.787.10^{12})^3}. \tag{36}$$

$$\mathbf{y}(\mathrm{s}) = \begin{bmatrix} 0.97(\mathrm{s}+0.95)10^6 \\ 8.827(\mathrm{s}+32.0)10^6 \end{bmatrix} \mathrm{r}(\mathrm{s}) \overline{(\mathrm{s}+294.0+1638.82\mathrm{i})(\mathrm{s}+294.0-1638.82\mathrm{i})(\mathrm{s}+0.0419)}.$$

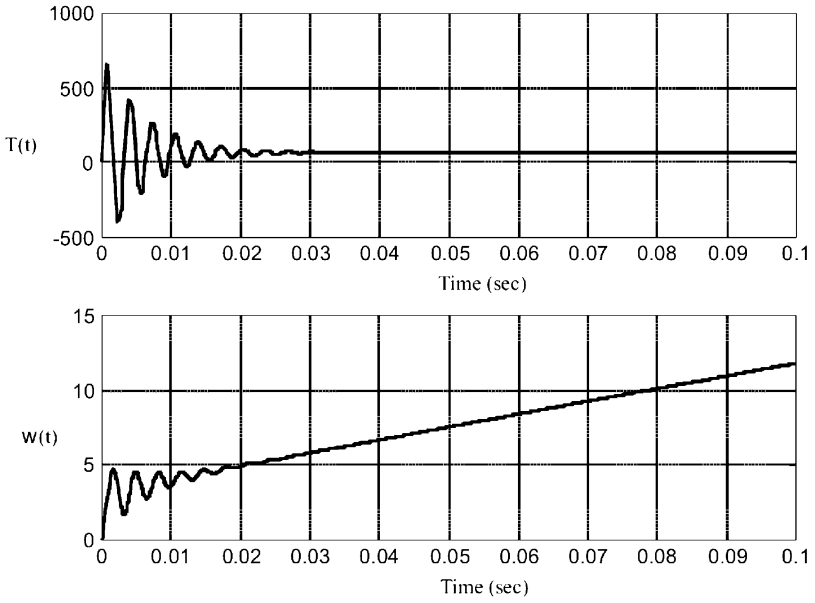

Fig. 4. Inner closed loop system response following a step change on $\mathrm{r}(\mathrm{t})$.

attained without the need for complicated decoupling pre-compensation or, in view of the restricted regulation energy available, integrators, as in [6]–[7].

The speed transient was also easily tuned using a phase lag filter of $f_2(\mathrm{s}) = (\mathrm{s}+500)/(\mathrm{s}+50)$ and a higher outer loop forward path, steady state gain of 0.6666. This resulted in smooth, monotonic changes in the gas generator compressor/turbine velocity and a rapidly decaying temperature transient, as shown in Fig. 5(b). The final closed loop transfer functions, if required could be estimated from these responses. Direct computation of the closed loop transfer function matrix would be difficult, computationally, owing to the time constant range of the system. Even simulation required the use of an initial small step size integration routine for "stiff" system models.

Closing each of the outer loops separately, does not lead to significantly, interactive output variations owing to the relatively long time transient of over 20.0 s being present in the speed response, shown in Fig. 4, with the inner loops closed. The effect of this time constant is largely absent from the temperature response of Fig. 4 owing to the inner loop, "near", pole-zero cancellation. As a consequence, following the closure of the inner loop, these two transients are distinctly different in character due to the effect of the dominant pole enabling single-loop techniques to be employed in the selection of the outer loop filters.

A simulation of the block diagram configuration for the combined system was used to obtain the transients of Fig. 5(a) and (b), excluding random noise disturbances and with $\mathrm{R}_1 = 1.3592$ and $\mathrm{R}_2 = 1.0$. The very low gains assigned to k_2 and h_2 had little discernable affect on the output transients and the simplified representation, shown in Fig. 6, could be employed for implementation purposes.

VIII. Conclusion

In this investigation the control of a small signal, linearized, automotive gas turbine model was considered. The model was obtained from measured, frequency response results from the actual system from which curve fitting procedures enabled a linearized, transfer function representation to be formulated.

The model, relating the two inputs of fuel flow $\mathrm{f}(\mathrm{t})$ and nozzle area change $\mathrm{n}(\mathrm{t})$ to the outputs of gas temperature and gas generator speed changes, was very poorly conditioned. The time constant range differed by a factor of 350.

A low-order approximation for the original model where remote singularities were neglected provided a simple analysis route. However, the gain disparity between column 1 and column 2 of the transfer matrix model remained, in view of the steady state output values. This had a marked influence on the inner loop design. Indeed the numerical values arising from the system model produced some extra ordinary ranges, as the analysis progressed.

In particular, the forward path gain ratio of $\mathrm{k}_1 = 1$ and $\mathrm{k}_2 = -8.0.10^{-6}$ and similarly, the measurement, feedback gains of $\mathrm{h}_1 = 2.8757$ and $\mathrm{h}_2 = -0.0009$ reflected this wide gain difference between columns 1 and 2 of the model.

These results for the inner loop feedback of the compensated system are in respect of the minimum control effort regulator. Generally, owing to the very high gains in column 1, of the transfer function matrix, the minimum effort regulator exercises control via this channel leaving the "k_2 channel" virtually unaffected.

In this way, the naturally occurring high gain paths through the system are exploited, minimizing thereby the amount of control effort and actuator activity which would be required in order to effect the required regulation.

This is true for any $\mathrm{b}(\mathrm{s})$ singularity and b_0 value. In selecting the $\mathrm{b}(\mathrm{s})$ function of sb_0 the sensitivity of the system was significantly reduced, when $\mathrm{b}_0 > 2.10^6$, as this expelled the troublesome poles to remote regions of the complex plane whilst forcing the system, with the inner loop closed, to behave predominantly as robustly stable, simple delays with a superimposed high frequency oscillation.

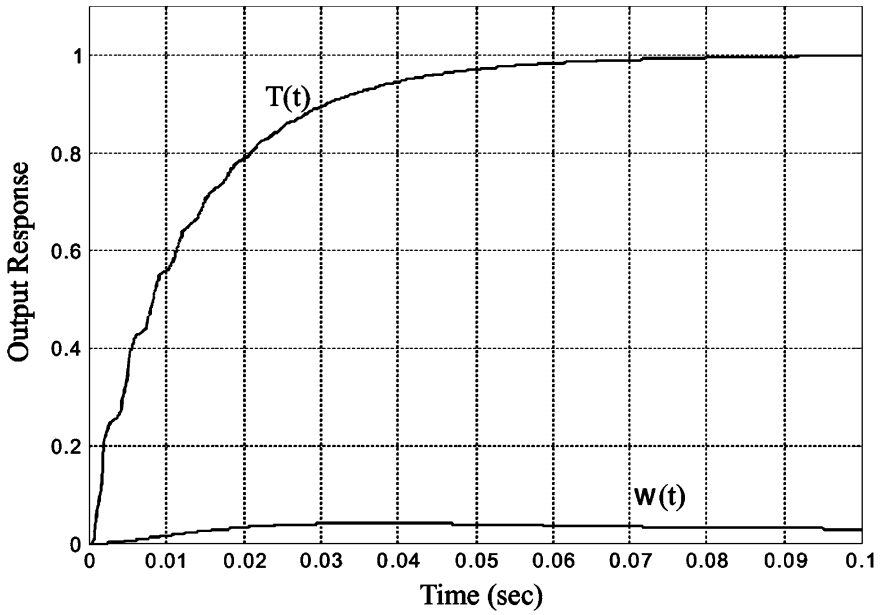

(a)

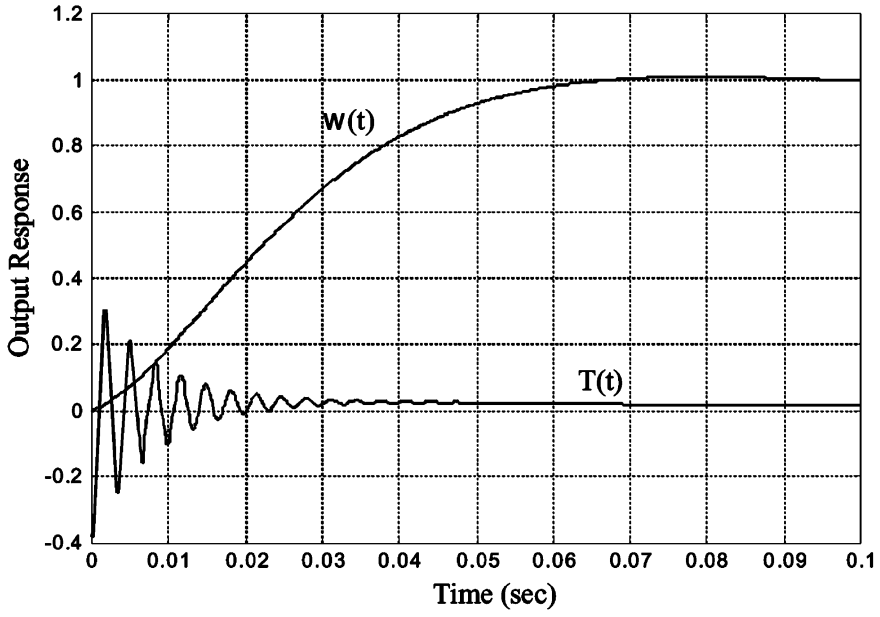

(b)

Fig. 5. (a) Output response following a step input change of unity on $\mathrm{r}_1(\mathrm{t})$. (b) Output response following a step input change of unity on $\mathrm{r}_2(\mathrm{t})$.

Closing the outer loops sequentially thereafter was relatively simple. The closure of loop 1 required two simple filters in cascade to achieve the fast, well behaved response shown in Fig. 5(a) and (b). Upon closing the second loop a phase lag filter was required owing to the residual output oscillation on the temperature characteristic leaving the principal gas generator speed response smooth, monotonic and sufficiently fast, for automotive applications, as shown in Fig. 5(b).

Finally, simplification of the control system block diagram, which would result in a more economical configuration, was explored via the simulation study. Essentially, this confirmed that the very small gains on k_2 and h_2 could be disregarded so that the inner loop feedback reduces to $\mathrm{k}_1(\mathrm{s})\mathrm{h}_1(\mathrm{s})$ as shown in Fig. 6.

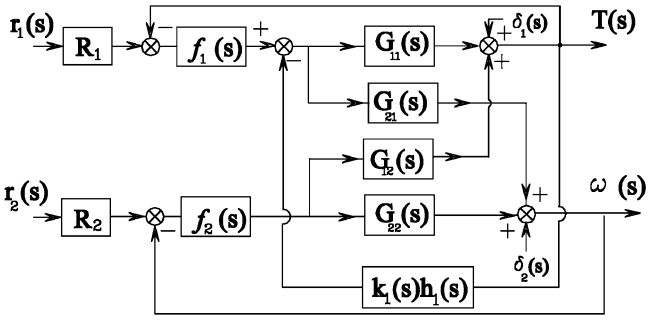

Fig. 6. Block diagram of final closed loop system for implementation purposes.

REFERENCES

[1] D. E. Winterbone, N. Munro, and P. M. G. Lourtie, "A preliminary study of the design of a controller for an automotive gas turbine," *Proc. ASME Gas Turbine Conference*, pp. 244–250, 1973. paper 73-GT-14.

[2] D. E. Winterbone, N. Munro, and P. M. G. Lourtie, "Design of a multivariable controller for an automotive gas turbine," in *IFAC Multivariable Symposium*, Manchester, U.K., 1974, pp. 1–4.

[3] J. Acurio, "Small gas turbines in the 21st century," *Soc. Auto. Eng.*, 1993.

[4] R. Whalley, "The computation of 2D transfer functions," in *Proc. I. Mech. E pt I*, vol. 205, 1991, pp. 59–67.

[5] B. D. Bunday, *Basic Optimization Methods*. London, U.K.: Edward Arnold, 1984.

[6] R. V. Patel and N. Munro, *Multivariable System Theory and Design*. London, U.K.: Academic, 1982.

[7] J. O. O'Reilly and W. E. Leithead, "Multivariable control by individual channel design," *Int J. Control*, vol. 54, no. 1, pp. 1–46, 1991.